ELSEVIER

11 August 1995

Chemical Physics Letters 242 (1995) 113–120

CHEMICAL
PHYSICS
LETTERS

Isolation of $H_2S \ldots ClF$ in a pre-reactive mixture of H_2S and ClF expanded in a coaxial jet and characterisation by rotational spectroscopy

H.I. Bloemink [a], K. Hinds [a], J.H. Holloway [b], A.C. Legon [a]

[a] *Department of Chemistry, University of Exeter, Stocker Road Exeter EX4 4QD, UK*
[b] *Department of Chemistry, University of Leicester, University Road, Leicester LE1 7RH, UK*

Received 25 May 1995; in final form 15 June 1995

Abstract

The reaction between H_2S and ClF was precluded and $H_2S \ldots ClF$ isolated by a coaxial supersonic expansion of the gaseous components into the Fabry–Pérot cavity of a pulsed-nozzle, Fourier-transform microwave spectrometer. The ground-state rotational spectra of seven isotopomers of $H_2S \ldots ClF$ were analysed and gave in each case the spectroscopic constants $\frac{1}{2}(B_0 + C_0)$, D_J, χ_{aa} (Cl) and M_{bb} (Cl). Interpretation of these constants revealed the complex to have a geometry of C_s symmetry with the S…Cl–F nuclei collinear in the order shown, with the angle $180° - \phi = 84.2(4)°$ between the C_2 axis of H_2S and the S…Cl–F axis, and with $r(S \ldots Cl) = 2.857(3)$ Å.

1. Introduction

We report the ground-state rotational spectra of seven isotopomers of a complex formed between H_2S and ClF. Although the reactions of various interhalogens with H_2S have been studied, that involving ClF does not appear to have been examined. In general, the interhalogens, XY, have properties intermediate between those of the parent halogens. The rapid reactions of F_2 and Cl_2 with H_2S to give HF or HCl and sulphur halides have been known for many years (i.e. since 1891 and 1825, respectively) [1]. Hence, it can be assumed that, when H_2S and ClF are mixed in the gas phase at normal temperatures and pressures, the reaction is vigorous. Nevertheless, by using a fast-mixing nozzle [2] in our pulsed-nozzle, Fourier-transform microwave spectrometer, it has been possible to arrest the reaction at the stage where the components form an encounter complex and then to characterise this transient species.

We embarked on this investigation for two reasons. The first was to establish, with a suitable example, that the fast-mixing nozzle is an effective means of isolating pre-chemical intermediates even when the Lewis base/halogen combination is violently reactive in static gas mixtures. The second reason for interest in $H_2S \ldots ClF$ arises from the rôle of this complex as a member of the series B…XY, where B is a Lewis B and XY is a halogen or interhalogen molecule. So far several members of the series $B \ldots Cl_2$ [3] and the series B…BrCl [4] have been characterised by means of their rotational spectra. The aim in each case has been to identify family relationships and systematic trends in several properties of B…XY as B is varied. In this way it has

SSDI 0009-2614(95)00694-X

been possible to detect patterns among, and draw general conclusions about, angular geometries, radial geometries, intermolecular binding strengths (as measured by k_{σ}, the intermolecular stretching force constant), and the extent of electric charge rearrangement in the XY subunit that attends formation of B...XY [3,4]. Of the series B...ClF, until recently only the case of B = HF could be examined in this way [5] because HF is one of the few substances (apart from the rare gases) that can coexist with ClF. The present investigation represents the first isolation of a gas-phase complex in a system B/ClF that is reactive.

2. Experimental

Rotational transitions of H_2S...ClF were observed with a pulsed-nozzle, Fourier-transform microwave spectrometer [6,7]. The reaction between H_2S and ClF was precluded by keeping the components separate until they expanded into the vacuum chamber of the spectrometer. This was achieved with a fast-mixing nozzle [2] attached to the outlet of a Series 9 (General Valve Corp.) solenoid valve. H_2S (Matheson Inc.) was flowed continuously through the central glass capillary (0.3 mm nominal internal diameter) into the vacuum chamber to give a background pressure of $\approx 1 \times 10^{-4}$ mbar while a mixture composed of 1% ClF in argon held in a stainless steel tank at ≈ 3 bar was pulsed via the solenoid valve down the outer of the two concentric, coterminal tubes that constitute the fast-mixing nozzle. Complexes H_2S...ClF were formed at the cylindrical interface of the emergent gas and their rotational spectrum was then recorded in the usual way. We found no evidence of HF produced in the reaction of H_2S and ClF when monitoring the $J = 1 \leftarrow 0$ transition of Ar...HF. Individual Cl-nuclear quadrupole hyperfine components in transitions of H_2S...ClF had a full-width at half-height of ≈ 15–20 kHz (see Fig. 1) and their frequencies were measured with an estimated accuracy of 2 kHz. For isotopomers containing D, additional broadening/partially resolved structure arising from D-nuclear quadrupole coupling resulted in larger errors.

Chlorine monofluoride, ClF, was prepared by the direct reaction of equimolar quantities of ClF_3 and Cl_2 [8] in the presence of CsF in a prefluorinated nickel reactor fitted with an Autoclave Engineers 316 ss valve (30 VM Series). After cooling to −196°C traces of non-condensables were pumped away. The products of reaction were separated by fractional condensation through traps at −142°C (methylcyclopentane slush) and −196°C, the ClF being collected and stored above the CsF in the original reactor. Mixtures of $HDS/H_2S/D_2S$ or pure D_2S were prepared by dropping an appropriate H_2O/D_2O mixture or pure D_2O, respectively, onto aluminium sulphide (Aldrich) in vacuo.

3. Results

3.1. Spectral analysis

The form of the observed rotational spectrum of each isotopomer of H_2S...ClF investigated was that expected for the ground state of a very nearly prolate asymmetric-top molecule having a large rotational constant A_0 and a significant a-component of the electric dipole moment. Thus, only the set of equally spaced transitions $(J+1)_{0,J+1} \leftarrow J_{0,J}$ was detected

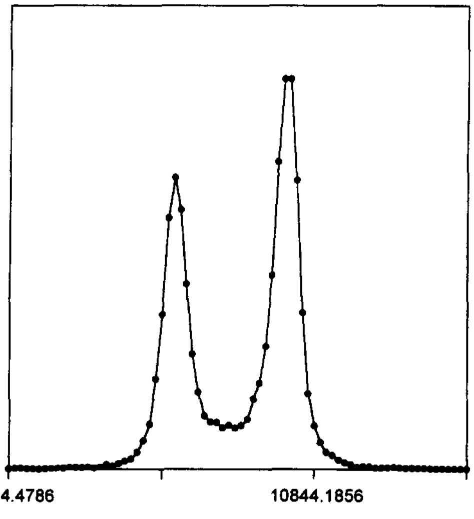

Fig. 1. A frequency domain record of the $F = {}^5/_2 \leftarrow {}^3/_2$ and $F = {}^3/_2 \leftarrow {}^1/_2$ nuclear quadrupole hyperfine components in the $3_{03} \leftarrow 2_{02}$ transition of $H_2{}^{32}S...{}^{35}ClF$. The signals from 70 gas pulses were averaged to obtain the spectrum, in which the dots are spaced by 3.90625 kHz.

for each isotopomer, their assignment confirmed by the characteristic Cl-nuclear quadrupole hyperfine splitting pattern. Detailed arguments, set out below and based on the spectroscopic constants of the seven isotopomers $H_2{}^{32}S\ldots{}^{35}ClF$, $H_2{}^{32}S\ldots{}^{37}ClF$, $H_2{}^{34}S\ldots{}^{35}ClF$, $HD^{32}S\ldots{}^{35}ClF$, $D_2{}^{32}S\ldots{}^{35}ClF$, $HD^{32}S\ldots{}^{37}ClF$ and $D_2{}^{32}S\ldots{}^{37}ClF$, demonstrate that the geometry of the complex is of the type shown in Fig. 2, with the $S\ldots ClF$ nuclei collinear or nearly so and with the angle $\phi = 95.8(4)°$. The determined geometry predicts the rotational constants $A = 141415$ MHz, $B = 1809.9$ MHz and $C = 1808.4$ MHz for the isotopomer $H_2{}^{32}S\ldots{}^{35}ClF$ and hence Ray's asymmetry parameter $\kappa = -0.99998$. A careful search in the predicted frequency range revealed none of the a-type R-branch transitions having $K_{-1} \geqslant 1$ expected of a molecule with this geometry, a result that can be understood when it is recognised that these levels lie at least 4.7 cm^{-1} in wavenumber above the corresponding $K_{-1} = 0$ level and would suffer rotational cooling to ~ 1 K in the supersonic expansion.

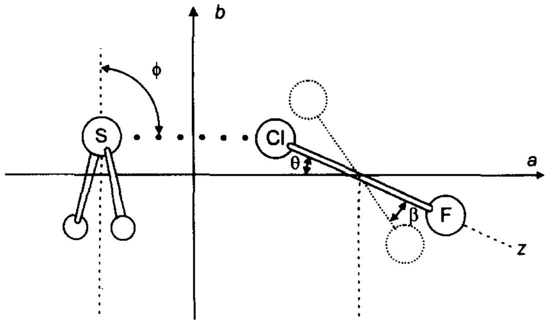

Fig. 2. Definition of the angles ϕ, and θ and β used in the discussion of the geometry and zero-point motion of $H_2S\ldots ClF$. The angle β describes the zero-point oscillation of the ClF subunit with respect to its own centre of mass in the parent isotopomer.

Observed frequencies of Cl-nuclear quadrupole hyperfine components in the transitions $(J+1)_{0,J} \leftarrow$

Table 1
Observed and calculated transition frequencies of $H_2{}^{32}S\ldots{}^{35}ClF$, $H_2{}^{32}S\ldots{}^{37}ClF$ and $H_2{}^{34}S\ldots{}^{35}ClF$

$J' \leftarrow J''$	$F' \leftarrow F''$	$H_2{}^{32}S\ldots{}^{35}ClF$		$H_2{}^{32}S\ldots{}^{37}ClF$		$H_2{}^{34}S\ldots{}^{35}ClF$	
		ν_{obs} (MHz)	$\Delta\nu$ (kHz) [a]	ν_{obs} (MHz)	$\Delta\nu$ (kHz) [a]	ν_{obs} (MHz)	$\Delta\nu$ (kHz) [a]
$2^{02} \leftarrow 1_{01}$	$3/2 \leftarrow 1/2$	7198.5045	−0.6	7179.6618	−0.1	–	–
	$5/2 \leftarrow 5/2$	72.01.5123	0.2	7182.0447	0.5	–	–
	$3/2 \leftarrow 5/2$	7227.3646	−1.2	–	–	–	
	$1/2 \leftarrow 1/2$	7234.3831	0.1	7207.9584	0.4	–	–
	$5/2 \leftarrow 3/2$	7237.4723	−2.4	7210.3903	–	–	
	$7/2 \leftarrow 5/2$	7237.5003	2.4	7210.4116	2.2	–	–
	$3/2 \leftarrow 3/2$	7263.3278	−0.7	7230.7467	−0.2	–	–
	$1/2 \leftarrow 3/2$	7299.2058	−0.5	7259.0429	−0.2	–	–
$3_{03} \leftarrow 2_{02}$	$7/2 \leftarrow 7/2$	10817.1870	0.4	10784.8043	−0.3	10497.8102	1.1
	$5/2 \leftarrow 7/2$	–	–	10798.0964	0.2	–	–
	$5/2 \leftarrow 3/2$	10844.2032	0.8	10806.1099	0.8	10524.8219	−0.4
	$3/2 \leftarrow 1/2$	10844.2750	−1.6	10806.1530	−2.0	10524.8970	−1.8
	$7/2 \leftarrow 5/2$	10853.1680	−4.5	10813.1747	4.8	10533.7889	−4.9
	$9/2 \leftarrow 7/2$	10853.1864	3.1	10813.1747	−2.3	10533.8069	2.1
	$5/2 \leftarrow 5/2$	10870.0562	0.0	10826.4607	−0.8	10550.6787	−1.7
	$3/2 \leftarrow 3/2$	10880.1545	0.1	10834.4525	1.4	10560.7735	0.6
	$3/2 \leftarrow 5/2$	10906.0086	0.4	–	–	–	–
$4_{04} \leftarrow 3_{03}$	$9/2 \leftarrow 9/2$	14433.4685	1.3	14388.0094	−0.4	–	–
	$7/2 \leftarrow 5/2$	14465.2576	−3.0	14413.0761	2.7	14039.4275	−2.0
	$5/2 \leftarrow 3/2$	14465.2875	8.0	14413.0761	−8.8	14039.4607	11.5
	$9/2 \leftarrow 7/2$	14469.4691	5.2	14416.3841	1.9	14043.6403	6.8
	$11/2 \leftarrow 9/2$	14469.4691	−1.3	14416.3841	14416.3841	14043.6403	0.2
	$7/2 \leftarrow 7/2$	14482.1452	0.9	14426.3643	−0.7	14056.3179	1.8
	$5/2 \leftarrow 5/2$	14501.2326	1.1	14441.4268	−0.1	–	–

[a] $\Delta\nu = \nu_{obs} - \nu_{calc}$.

Table 2
Observed and calculated transition frequencies of $D_2{}^{32}S\ldots{}^{35}ClF$, $D_2{}^{32}S\ldots{}^{37}ClF$, $HD^{32}S\ldots{}^{35}ClF$ and $HD^{32}S\ldots{}^{37}ClF$

$J' \leftarrow J''$	$F \leftarrow F''$	$D_2{}^{32}S\ldots{}^{35}ClF$		$D_2{}^{32}S\ldots{}^{37}ClF$		$HD^{32}S\ldots{}^{35}ClF$		$HD^{32}S\ldots{}^{37}ClF$	
		ν_{obs} (MHz)	$\Delta\nu$ (kHz) [a]	ν_{obs} (MHz)	$\Delta\nu$ (kHz) [a]	ν_{obs} (MHz)	$\Delta\nu$ (kHz) [a]	ν_{obs} (MHz)	$\Delta\nu$ (kHz) [a]
$3_{03} \leftarrow 2_{02}$	$7/2 \leftarrow 7/2$	10450.6631	0.6	10416.1058	0.1	10628.7679	0.1	–	–
	$7/2 \leftarrow 5/2$	10486.6172	11.7	10444.4461	7.5	10664.7437	12.8	–	–
	$9/2 \leftarrow 7/2$	10486.6172	0.9	10444.4461	0.0	10664.7437	2.2	10623.6185	0.2
	$5/2 \leftarrow 5/2$	10503.4726	−1.5	10457.7160	−0.1	10681.6056	−2.4	10636.8977	−0.2
$4_{04} \leftarrow 3_{03}$	$9/2 \leftarrow 9/2$	–	–	–	–	14182.2438	−0.2	–	–
	$7/2 \leftarrow 5/2$	13976.5260	−3.8	13921.4560	−1.7	14214.0103	−6.6	14160.3566	−4.5
	$5/2 \leftarrow 3/2$	13976.5657	16.0	13921.4753	5.9	14214.0502	13.5	14160.3566	3.9
	$9/2 \leftarrow 7/2$	13980.7368	8.0	13924.7666	3.2	14218.2225	4.7	14163.6446	−1.9
	$11/2 \leftarrow 9/2$	13980.7368	1.6	13924.7666	−1.5	14218.2225	−1.5	14163.6528	2.5
	$7/2 \leftarrow 7/2$	13993.4002	1.8	–	–	14230.8995	5.6	–	–
	$5/2 \leftarrow 5/2$	14012.4604	0.3	–	–	14249.9662	−2.0	–	–

[a] $\Delta\nu = \nu_{obs} - \nu_{calc}$.

$J_{0,J}$ for $J = 1$, 2, 3 are recorded in Table 1 for the isotopomers $H_2{}^{32}S\ldots{}^{35}ClF$ and $H_2{}^{32}S\ldots{}^{37}ClF$ together with those for $J = 2$, 3 for the isotopomer $H_2{}^{34}S\ldots{}^{35}ClF$ measured in natural abundance. The frequencies for the $J = 2$ and $J = 3$ transitions of $HD^{32}S\ldots{}^{35}ClF$, $HD^{32}S\ldots{}^{37}ClF$, $D_2{}^{32}S\ldots{}^{35}ClF$ and $D_2{}^{32}S\ldots{}^{37}ClF$ are given in Table 2. The high consumption of HDS and D_2S when employed in continuous flow through the fast-mixing nozzle restricted the number of transitions that could be measured for isotopomers containing deuterium.

It is readily shown [9] for a molecule of $\kappa = -0.99998$ that the frequencies of transitions $(J+1)_{0,J+1} \leftarrow J_{0,J}$ can be fitted to within our experimental accuracy by using a Hamiltonian appropriate to a linear or $K = 0$ symmetric-top molecule. The form employed was

$$H = \tfrac{1}{2}(B_0 + C_0)\boldsymbol{J}^2 - D_J\boldsymbol{J}^4 - \tfrac{1}{6}\mathbf{Q}(\mathrm{Cl}):\boldsymbol{\nabla E}(\mathrm{Cl}) - \boldsymbol{I}(\mathrm{Cl}) \cdot \mathbf{M}(\mathrm{Cl}) \cdot \boldsymbol{J}, \qquad (1)$$

where the first two terms have their conventional meanings, the third term describes the Cl-nuclear quadrupole interaction while the fourth accounts for the additional shifts in the hyperfine levels brought about by magnetic coupling of the Cl-nuclear spin vector $\boldsymbol{I}(\mathrm{Cl})$ to $\boldsymbol{J}$. In a standard interative least squares fit of the observed hyperfine frequencies, the matrix of H was constructed in the coupled basis $\boldsymbol{I}(\mathrm{Cl}) + \boldsymbol{J} = \boldsymbol{F}$ and diagonalized in blocks of F. The only spectroscopic constants determinable from the data were $\frac{1}{2}(B_0 + C_0)$, D_J, $\chi_{aa}(\mathrm{Cl}) = -[eQ(\mathrm{Cl})/h]\partial^2 V/\partial a^2$ and the component $M_{bb}(\mathrm{Cl})$ of the chlorine spin–rotation coupling tensor $\mathbf{M}(\mathrm{Cl})$. Values of these constants from the final cycles of the fits are recorded in Table 3 while the residuals $\Delta\nu = \nu_{obs} - \nu_{calc}$ are shown in Tables 1 and 2. The standard deviation σ of the fit (see Table 3) was less than the estimated error of frequency measurement for all isotopomers based on H_2S and establishes the adequacy of the Hamiltonian employed. For some of

Table 3
Ground-state spectroscopic constants of seven isotopomers of $H_2S\ldots ClF$

	$H_2{}^{32}S\ldots{}^{35}ClF$	$H_2{}^{32}S\ldots{}^{37}ClF$	$H_2{}^{34}S\ldots{}^{35}ClF$	$D_2{}^{32}S\ldots{}^{35}ClF$	$D_2{}^{32}S\ldots{}^{37}ClF$	$HD^{32}S\ldots{}^{35}ClF$	$HD^{32}S\ldots{}^{37}ClF$
$\frac{1}{2}(B_0 + C_0)$ (MHz)	1808.6137(2)	1802.0071(2)	1755.3826(2)	1747.5164(3)	1740.5486(2)	1777.2056(5)	1770.4131(6)
D_J (kHz)	2.111(6)	2.098(5)	2.040(7)	1.936(9)	1.903(9)	2.03(2)	2.03(2)
$\chi_{aa}(\mathrm{Cl})$ (MHz)	−144.002(2)	−113.492(2) −144.009(6) [a]	−144.001(3)	−143.838(3)	−113.362(3) −143.844(7) [a]	−143.919(5)	−113.42(2) −143.92(3) [a]
$M_{bb}(\mathrm{Cl})$ (kHz)	−2.1(2)	−1.7(1)	−2.1(2)	−1.8(2)	−1.9(2)	−1.7(3)	−1.0(5)
σ (kHz) [b]	1.6	1.5	2.0	2.8	2.8	4.8	4.7

[a] The observed $\chi_{aa}({}^{37}\mathrm{Cl})$ multiplied by the ratio $Q({}^{35}\mathrm{Cl})/Q({}^{37}\mathrm{Cl}) = 1.26889(3)$, given in Ref. [21].

[b] σ are the standard deviations of the fits reported in Tables 1 and 2.

the deuteriated isotopomers the slightly poorer fit can be attributed to an additional (but only partially resolved) hyperfine structure in some transitions arising from the D-nuclear quadrupole interaction, which increased the error of frequency measurement.

3.2. Molecular geometry

The changes in $\frac{1}{2}(B_0 + C_0)$ accompanying isotopic substitution in $H_2{}^{32}S \ldots {}^{35}ClF$ establish that the heavy atoms lie in the order S...Cl–F. Arguments concerned with the changes in the magnitude of $\chi_{aa}(Cl)$ on substitution of ^{34}S or D_2 in $H_2{}^{32}S \ldots {}^{35}ClF$ given in Section 3.3 show that the S...Cl–F nuclei must be collinear to within a degree or two in the equilibrium geometry. In what follows, we take the heavy atoms as collinear and then demonstrate that our geometrical conclusions are relatively insensitive to deviations of the S...Cl–F angle from 180° by ± 10°.

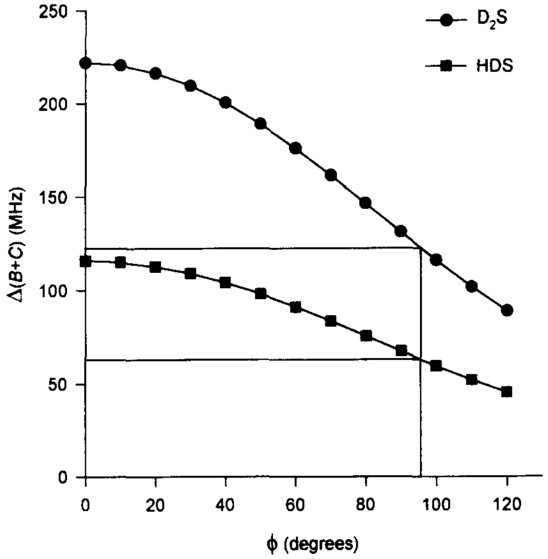

Fig. 3. $\Delta(B+C)$ versus the angle ϕ for $HD^{32}S \ldots {}^{35}ClF$ and $D_2{}^{32}S \ldots {}^{35}ClF$. $\Delta(B+C)$ is the difference in $B+C$ between the parent isotopomer $H_2{}^{32}S \ldots {}^{35}ClF$ and the isotopically substituted species $HD^{32}S \ldots {}^{35}ClF$ or $D_2{}^{32}S \ldots {}^{35}ClF$ calculated at the given angle ϕ and at the $r(S \ldots Cl)$ that reproduces $B_0 + C_0$ for the parent isotopomer. The horizontal lines indicate the observed values of $B_0 + C_0$ for $HD^{32}S \ldots {}^{35}ClF$ and $D_2{}^{32}S \ldots {}^{35}ClF$.

In view of the relatively weak interaction of H_2S and ClF (as established in Sections 3.3 and 3.4), we assume the r_0-geometries of H_2S [10] and ClF [11] shown in Table 4 survive complex formation. Then, only the distance $r(S \ldots Cl)$ and the angle ϕ are required to define the geometry of $H_2S \ldots ClF$ if the heavy atoms are collinear. To fit $r(S \ldots Cl)$ and ϕ the following procedure was employed. For a given angle ϕ, the distance $r(S \ldots Cl)$ was adjusted until the observed value of $B_0 + C_0$ for $H_2{}^{32}S \ldots {}^{35}ClF$ was reproduced. With this geometry, the changes $\Delta(B+C)$ accompanying single and double substitution of H by D were then calculated. By repeating the approach for small increments of ϕ in the range $\phi = 0$ to 120°, the curves of $\Delta(B+C)$ versus ϕ for $HDS \ldots {}^{35}ClF$ and $D_2{}^{32}S \ldots {}^{35}ClF$ shown in Fig. 3 were generated. The experimental values of $\Delta(B_0 + C_0)$ for single and double D substitution in $H_2{}^{32}S \ldots {}^{35}ClF$ are also indicated in Fig. 3 and lead to $\phi = 95.7(4)°$ and $95.9(4)°$, respectively, where the error is in each case that resulting from repeating the calculation by assuming the S...Cl–F nuclei differ from collinearity by + 10° and − 10°. The corre-

Table 4
Spectroscopic and geometric properties of H_2S and ClF

	A_0 (MHz)	B_0 (MHz)	C_0 (MHz)	χ_0(Cl) (MHz)	Geometry
$H_2{}^{32}S$ [a]	310182.24	270884.05	141705.88		
$H_2{}^{34}S$ [b]	309101.1	270884.0	141470.3		∠HSH = 92.13°
HDS [a]	292351.30	147861.80	96704.12		r_0(S–H) = 1.3518 Å
D_2S [a]	164571.12	135380.31	73244.07		
^{35}ClF		15418.251 [c]	15418.251 [c]	− 145.8718 [d]	r_0 = 1.63176 Å [e]
^{37}ClF		15125.652 [c]	15125.652 [c]	− 114.9613 [d]	r_0 = 1.63173 Å [e]

[a] Ref. [10]. [b] Calculated from the r_0 geometry in the final column.
[c] Ref. [11]. [d] Ref. [13]. [e] Calculated from B_0 values.

Table 5
Some properties of $H_2S\ldots ClF$

Isotopomer	$\Delta(\frac{1}{2}(B+C))$ (MHz) [a]	k_σ ($N\,m^{-1}$) [b]
$H_2{}^{32}S\ldots{}^{35}ClF$	0.00	13.38(4)
$H_2{}^{32}S\ldots{}^{37}ClF$	0.47	13.47(3)
$H_2{}^{34}S\ldots{}^{35}ClF$	1.20	13.16(5)
$HD^{32}S\ldots{}^{35}ClF$	−0.03	13.29(13)
$D_2{}^{32}S\ldots{}^{35}ClF$	0.06	13.61(6)
$HD^{32}S\ldots{}^{37}ClF$	0.44	13.34(13)
$D_2{}^{32}S\ldots{}^{37}ClF$	0.53	13.85(6)

[a] $\frac{1}{2}(B_0+C_0)_{obs} - \frac{1}{2}(B+C)_{calc}$. See text for discussion.

[b] Calculated using Eq. (5) and spectroscopic constants from Tables 3 and 4. The error is that generated from the error in D_J. There are systematic errors arising from the model used to obtain Eq. (5).

sponding distances $r(S\ldots Cl)$ are 2.857(3) and 2.857(3) Å, respectively. When the mean of the collinear geometries is used to calculate $\frac{1}{2}(B+C)$ for all observed isotopomers, there is excellent agreement with the experimental values, as illustrated in Table 5. In an alternative approach, a fit of $\frac{1}{2}(B_0+C_0)$ for all seven isotopomers simultaneously gave $\phi = 95.7(3)°$ and $r(S\ldots Cl) = 2.8566(4)$ Å for collinear S...Cl–F nuclei. Clearly, the angular geometry of $H_2S\ldots ClF$ is well established.

The conclusion that there is a steeply pyramidal configuration at S is also consistent with the failure to resolve inversion doubling in spectral transitions that would result from tunnelling between equivalent forms and with the failure to observe a-type, R-branch transitions having $K_{-1} = 1$. In a detailed argument set out elsewhere [12], it was noted that transfer of population from the higher energy $K_{-1} = 1$ states to $K_{-1} = 0$ states in complexes $H_2Y\ldots HX$ (Y = O, S and X is a halogen) can occur during supersonic expansion in a pulsed jet experiment only if the H_2Y protons cannot be exchanged by a rotation C_2^a about the a axis, i.e. only if the component μ_c of the electric dipole moment operator is non-zero. This restriction results because the population transfer corresponds to a forbidden collisional interconversion between $I = 1$ and $I = 0$ spin states of the H_2Y protons in the cases where $\mu_c = 0$. Thus $H_2O\ldots HCl$, which is effectively planar and therefore has vibrational wavefunctions of C_{2v} symmetry, exhibits $K_{-1} = 1$ transitions with a room temperature intensity relative to $K_{-1} = 0$ transitions, despite supersonic expansion. The absence of $K_{-1} = 1$ transitions and inversion doubling in $H_2S\ldots ClF$, as in $H_2S\ldots HCl$ [9], is therefore evidence in support of a permanently nonplanar, C_s geometry for the former also.

3.3. Interpretation of $\chi_{aa}(Cl)$

The observed value of $\chi_{aa}(Cl)$ (see Table 3) differs from $\chi_0(Cl) = -145.872$ MHz of free ClF [13] for three reasons. First, the electric field gradient at Cl along the ClF axis (z) is modified when the H_2S subunit achieves its equilibrium position in the complex and the corresponding coupling constant becomes $\chi_0'(Cl)$. The effect of the Lewis base B in complexes $B\ldots Cl_2$ is to increase the magnitude of $\chi_0'(Cl)$ of the inner nucleus [14] and presumably this will be so for Cl in $H_2S\ldots ClF$. Secondly, the equilibrium component $\chi_{aa}^e(Cl)$ of the Cl-nuclear quadrupole coupling tensor of $H_2S\ldots ClF$ is given by the projection of $\chi_0'(Cl)$ through the angle θ onto the a axis (see Fig. 2), so that

$$\chi_{aa}^e(Cl) = \chi_0'(Cl) P_2(\cos\theta). \qquad (2)$$

Finally, the angular oscillation β of the ClF subunit with respect to its centre of mass (see Fig. 2 for definition) can be taken into account, in the approximation that $\chi_0'(Cl)$ does not vary significantly with β, by the projection term $\langle P_2(\cos\beta)\rangle$ to give the zero-point value

$$\chi_{aa}(Cl) = \chi_0'(Cl) P_2(\cos\theta)\langle P_2(\cos\beta)\rangle. \qquad (3)$$

The isotopic variation of $\chi_{aa}(Cl)$ can be used to demonstrate that the S...Cl–F nuclei are within a degree or two of collinearity and that the term $P_2(\cos\theta)$ is negligibly different from unity. It is reasonable to assume that isotopic substitution in the H_2S subunit will leave $\langle P_2(\cos\beta)\rangle$ unaffected. If so, the entire change in $\chi_{aa}(Cl)$ that accompanies ^{34}S or D-substitution originates in the rotation of the a axis caused by the substitution, which changes θ to $\theta + \delta\theta$.

When the S...Cl–F nuclei are assumed collinear, the geometry obtained in Section 3.2 (namely, $r(S\ldots Cl) = 2.857(3)$ Å and $\phi = 95.8(4)°$) leads to $\theta = 0.787°$ for $H_2{}^{32}S\ldots{}^{35}ClF$ but substitution of ^{34}S causes an a-axis rotation, which decreases θ to 0.746°. The term $P_2(\cos\theta)$ will therefore increase from 0.99972 in $H_2{}^{32}S\ldots{}^{35}ClF$ to 0.99975 in

$H_2{}^{34}S\ldots{}^{35}ClF$. With the assumption that $\langle P_2(\cos\beta)\rangle$ in Eq. (3) is unchanged by this substitution, $\chi_{aa}(Cl)$ should increase by the ratio 0.99975/0.99972 from −144.002(2) MHz in $H_2{}^{32}S\ldots{}^{35}ClF$ to −144.006(2) MHz on ^{34}S substitution. The observed value for the ^{34}S isotopomer is 144.001(3) MHz (Table 3). On the other hand, a small deviation of the S...Cl–F nuclei from collinearity makes the agreement worse. For example, if the S...Cl–F angle were 183°, θ decreases from 2.990° in $H_2{}^{32}S\ldots{}^{35}ClF$ to 2.957° in $H_2{}^{34}S\ldots{}^{35}ClF$ and the corresponding argument leads to a prediction of $\chi_{aa}(Cl) = -144.015(2)$ MHz for the latter species.

The a-axis rotation on substitution of each H by D in $H_2{}^{32}S\ldots{}^{35}ClF$ is larger and allows a more positive conclusion. In the geometry with collinear heavy atoms, dideuterium substitution causes θ to increase from 0.787° to 1.503° and, correspondingly, $P_2(\cos\theta)$ to decrease from 0.99972 to 0.99897. Hence, the value of $\chi_{aa}(Cl)$ for $D_2{}^{32}S\ldots{}^{35}ClF$ is predicted to be −143.894(2) MHz, in reasonable agreement with the observed value −143.838(3) MHz (Table 3). However, when the S...Cl – F angle is 183°, the same analysis gives $\chi_{aa}(Cl) = -143.682(2)$ MHz which is significantly different from the observed value. It is clear that a departure of the S...Cl–F nuclei from collinearity by more than a degree or two can be ruled out. In that case $P_2(\cos\theta)$ differs negligibly from unity and it can be ignored in Eq. (3).

To obtain $\chi_0'(Cl)$ from Eq. (3), we then require only a value of $\langle P_2(\cos\beta)\rangle$. The force constant ($k_\sigma = 13.4$ N m^{-1}) for $H_2{}^{32}S\ldots{}^{35}ClF$ (see Section 3.4) is very similar to that ($k_\sigma = 12.7$ N m^{-1}) of $H_3N\ldots{}^{35}Cl_2$ [15]. The angle $\beta_{av} = \cos^{-1}\langle\cos^2\beta\rangle^{1/2} = 7.5°$ has been estimated from the Cl-nuclear quadrupole coupling constants of the latter molecule. If the similarity in k_σ implies that the hydrogen bond bending force constant k_β is similar for both molecules, a simple model [16] shows that β_{av} scales as $I_b^{1/4}$, where I_b is the moment of inertia of the ClF or Cl_2 subunit. This leads to a predicted value of $\beta_{av} = 9.0°$ for $H_2S\ldots{}^{35}ClF$ which allows $\chi_0'(^{35}Cl) \approx 150$ MHz to be obtained from Eq. (3). The important conclusion is that $\chi_0'(^{35}Cl)$ is increased in magnitude by only about 4 MHz from the free molecule value $\chi_0(^{35}Cl)$ (see Table 5). Evidently, formation of $H_2S\ldots ClF$ has not caused a significant electric charge redistribution within the ClF subunit.

3.4. Strength of the $H_2S\ldots ClF$ interaction

One measure of the strength of the interaction of H_2S and ClF in $H_2S\ldots ClF$ is the intermolecular stretching force constant k_σ. In the approximation of harmonic intermolecular modes of vibration and rigid subunits, the centrifugal distortion constant Δ_J of an asymmetric-rotor molecule (like $H_2S\ldots ClF$) in which a linear subunit is perpendicular to the plane of the nuclei of a planar subunit is related to k_σ by [17]

$$k_\sigma = (8\pi^2\mu/\Delta_J)\left[B_0^3(1 - B_0/B_{ClF} - B_0/B_{H_2S}) + C_0^3(1 - C_0/C_{ClF} - C_0/C_{H_2S})\right], \qquad (4)$$

where B_0 and C_0 refer to $H_2S\ldots ClF$ while B_{ClF}, B_{H_2S}, etc. refer to the rotational constants of the monomers [10,11] (see Table 4) and $\mu = m_{H_2S}m_{ClF}/(m_{H_2S} + m_{ClF})$. Because $B_0 - C_0$ is very small (≈ 1.5 MHz for $H_2{}^{32}S\ldots{}^{35}ClF$) and $B_0/B_{H_2S} \approx C_0/C_{H_2S} \approx 10^{-2}$, Eq. (4) can be written with negligible error as

$$k_\sigma = (2\pi^2\mu/\Delta_J)(B_0 + C_0)^3 \times (1 - B_0/B_{ClF} - B_0/B_{H_2S}). \qquad (5)$$

If D_J determined here can be used in place of Δ_J, the appropriate spectroscopic constants from Table 3 and Table 4 used in Eq. (5) lead to the values of k_σ given in Table 5 for the seven isotopomers of $H_2S\ldots ClF$ investigated. The range of values presumably reflects systematic deficiencies in the model rather than experimental error in D_J but we note that the range is sufficiently small to show that the interaction is relatively weak.

4. Discussion

A detailed analysis of the ground-state rotational spectra of seven isotopomers of $H_2S\ldots ClF$ has established that the angular geometry is of the type shown in Fig. 2, with $\phi = 95.8(4)°$ and the S...Cl–F nuclei collinear in the equilibrium conformation. This is very similar to those of $H_2S\ldots Cl_2$ ($\phi = 101(2)°$ [19]) and $H_2S\ldots BrCl$ ($\phi = 97(1)°$ [18]) and can likewise be interpreted in terms of a set of simple rules [20] for predicting angular geometries, as discussed elsewhere [3,4]. The stretching force constant k_σ provides a measure of the strength of binding, from which we note that $k_\sigma(H_2S\ldots ClF) \approx k_\sigma(H_2S\ldots BrCl) \approx 2k_\sigma(H_2S\ldots Cl_2)$. Evidently, the polar interhalogens lead to a greater binding strength than nonpolar Cl_2. Finally, we note that $r(S\ldots Cl)$ in $H_2S\ldots ClF$ is ≈ 0.4 Å shorter than in $H_2S\ldots Cl_2$ [19], even though the same atoms are primarily involved in the interaction.

Acknowledgements

We thank the EPSRC for a studentship (for KH) and a research grant in support of this work. Help with the preparation of ClF from Dr. E.G. Hope is gratefully acknowledged.

References

[1] Gmelin's Handbuch der Anorganischen Chemie, System 9, Main B1, Sulphur, Hydrides and Oxides (Springer, Berlin, 1953/1974) pp. 60, 66.

[2] A.C. Legon and C.A. Rego, J. Chem. Soc. Faraday Trans. 86 (1990) 1915.

[3] A.C. Legon, Chem. Phys. Letters 237 (1995) 291, and references therein.

[4] A.C. Legon, J. Chem. Soc. Faraday Trans. 91 (1995) 1881, and references therein.

[5] S.E. Novick, K.C. Janda and W. Klemperer, J. Chem. Phys. 65 (1976) 5115.

[6] T.J. Balle and W.H. Flygare, Rev. Sci. Instr. 52 (1981) 33.

[7] A.C. Legon, in: Atomic and molecular beam methods, Vol. 2, ed. G. Scoles (Oxford Univ. Press, Oxford, 1992) ch. 9.

[8] C.J. Schack and R.D. Wilson, Inorg. Synth. 24 (1986) 1.

[9] E.J. Goodwin and A.C. Legon, J. Chem. Soc. Faraday Trans. II 80 (1984) 51.

[10] R.L. Cook, F.C. Delucia and P. Helminger, J. Mol. Struct. 28 (1975) 237.

[11] J.C. McGurk, C.L. Norris, H.L. Tigelaar and W.H. Flygare, J. Chem. Phys. 58 (1973) 3, 118.

[12] A.C. Legon, Faraday Discussions Chem. Soc. 86 (1988) 269.

[13] B. Fabricant and J.S. Muenter, J. Chem. Phys. 66 (1977) 5274.

[14] P.W. Fowler, A.C. Legon and S.A. Peebles, unpublished observations.

[15] A.C. Legon, D.G. Lister and J.C. Thorn, J. Chem. Soc. Faraday Trans. 90 (1994) 3205.

[16] P. Cope, D.J. Millen and A.C. Legon, J. Chem. Soc. Faraday Trans. II 82 (1986) 1189.

[17] D.J. Millen, Can J. Chem. 63 (1983) 1477.

[18] H.I. Bloemink and A.C. Legon, unpublished observations.

[19] H.I. Bloemink, S.J. Dolling, K. Hinds and A.C. Legon, J. Chem. Soc. Faraday Trans. 91 (1995), in press.

[20] A.C. Legon and D.J. Millen, Faraday Discussions Chem. Soc. 73 (1982) 71; Chem. Soc. Rev. 16 (1987) 467.

[21] A.C. Legon and J.C. Thorn, Chem. Phys. Letters 215 (1993) 554.